Bulk crystal growth and optical properties of a novel organic–inorganic hybrid nonlinear optical thiocyanate: [Mn(CH₃CONH₂)₂] [Hg(SCN)₄]†

Peiqing Long,[a] Chunli Hu,[a] Xitao Liu [ID][a,b] and Jianggao Mao [ID]*[a,b]

The growth of bulk nonlinear optical (NLO) crystals that exhibit robust second harmonic generation (SHG) is currently an intriguing and rapidly advancing field for laser and photonic applications. Among the various options available, organic–inorganic hybrid materials offer numerous possibilities due to their distinctive amalgamation of inorganic coordinate frameworks and organic molecules. Herein, we have successfully developed a novel non-centrosymmetric (NCS) organic–inorganic hybrid NLO material, manganese mercury thiocyanate-bis(acetamide), [Mn(CH₃CONH₂)₂][Hg(SCN)₄] (MMTA), by synergistically incorporating inorganic polyhedra and organic conjugated molecules. The crystal displays a polar architecture comprising an asymmetric [HgS₄] tetrahedron and [MnN₄O₂] octahedron, which are connected by four π-conjugated −S−C≡N− ligands. More intriguingly, inch-sized single crystals with dimensions up to 50 × 50 × 12 mm³ have been easily grown from aqueous solutions by a temperature-lowering method. The optical property investigation suggests that MMTA is a phase-matching NLO material with a large SHG response approximately 2.5 times that of KH₂PO₄, demonstrating its potential for NLO applications. Based on a combination of structural analysis and theoretical calculations, it is suggested that the significant SHG response can be attributed to the cooperative interaction between conjugated organic molecules and a highly asymmetric inorganic distorted octahedron. This work introduces an effective approach for the discovery of high-performance quadratic NLO materials, with a particular focus on organic–inorganic hybrid compounds.

Introduction

Nonlinear optical (NLO) crystals, which play a vital role as essential materials in solid-state optical devices, are in great demand in laser and photonic technologies.[1–3] Particularly, quadratic NLO materials have gained considerable interest due to their ability to greatly expand the wavelength spectrum of solid-state lasers *via* cascaded second harmonic generation (SHG), rendering them extremely valuable for a wide range of applications, such as laser-based medical procedures, precision material shaping, advanced photolithography techniques, *etc.*[4–10] Despite ongoing efforts, discovering and designing novel NLO materials remains a challenge, primarily owing to the requirement of a non-centrosymmetric (NCS)

structure.[11] To achieve NCS structures necessary for NLO properties, a commonly employed approach involves utilizing second-order Jahn–Teller (SOJT) cations including Pb²⁺, Sn²⁺, Bi³⁺ and Sb³⁺ that disrupt crystalline symmetry through induced distorted polyhedra.[12–14] In addition, it is important to mention that several groundbreaking studies have proposed the effectiveness of planar π-conjugated groups including inorganic BO₃²⁻, CO₃²⁻ and NO₃⁻ and organic π-conjugated benzene-like groups[8,15–18] in inducing a significant SHG response. As a result, significant endeavors have been devoted to the search for NLO materials in recent years, resulting in continuous advancements in the discovery of NLO crystals across various material systems including phosphates,[19] sulfates,[20] nitrates,[21] carbonates,[8] selenites,[22] and cyanurate salts,[23] among others. Some of these discoveries hold promising potential as candidates for future generations of NLO materials.

Organic–inorganic hybrid materials, being a burgeoning category of optoelectronic materials with flexible crystal structures and multifunctional properties, have been extensively investigated.[24–29] In particular, the inherent advantages of organic cations and inorganic metal ions can be effectively

[a]State Key Laboratory of Functional Crystals and Devices, Fujian Institute of Research on the Structure of Matter, Chinese Academy of Sciences, Fuzhou, Fujian 350002, China. E-mail: mjg@fjirsm.ac.cn
[b]University of Chinese Academy of Sciences, Beijing 100049, China

harnessed to create exceptional NLO materials with unparalleled performance. Among them, metal thiocyanates are particularly important due to the presence of lone electron pairs on sulfur (S) and nitrogen (N), which contribute to their strong polarizability.[3,30] However, despite these favorable characteristics, thiocyanates have largely been overlooked in NLO research. Metal thiocyanate crystals with the composition AB (SNC)$_4$ (such as MnHg(SCN)$_4$, CdHg(SCN)$_4$, ZnHg(SCN)$_4$ and ZnCd(SCN)$_4$) have attracted attention from crystallographers as they meet most requirements for efficient NLO crystals.[31–35] Additionally, another series of thiocyanate NLO materials AB (SCN)$_4$(L)$_2$ (A = Hg; B = Mn, Cd; L = dimethyl sulfoxide, glycol monomethyl ether or N-methylformamide), which incorporate SCN ions and L acting as a ligand with potential S and N donors into their crystal structure, have also shown interesting NLO properties.[36–39] However, the overall performance of these compounds is unsatisfactory; particularly, the challenges in growing large single crystals hinder their further applications. For instance, the MnHg(SCN)$_4$ crystal demonstrates a significant SHG response, which is several dozen times greater than that of the KH$_2$PO$_4$ (KDP) crystal; however, the growth of bulk single crystals is hindered by defects during the crystallization process.[31] Therefore, it is crucial to explore novel NLO materials with excellent comprehensive performance through rational design in the thiocyanate system.

It is known that planar π-conjugated units, including acylamino groups, have been extensively employed in the design and synthesis of NLO materials due to their enhanced electron delocalization and charge transfer interactions.[3] Inspired by these results, herein, we have successfully developed a noncentrosymmetric (NCS) organic–inorganic hybrid NLO material, manganese mercury thiocyanate-bis(acetamide), [Mn(CH$_3$CONH$_2$)$_2$][Hg(SCN)$_4$] (MMTA), by synergistically incorporating inorganic polyhedra and organic acetamide units containing acylamino moieties. The temperature-lowering method was employed to grow inch-sized MMTA single crystals with dimensions up to 50 × 50 × 12 mm^3, which exhibit a significantly large SHG response approximately 2.5 times greater than that of KDP. Moreover, these crystals possess a wide transmission window from 360 to 2500 nm, showcasing their potential for diverse NLO applications. These results present an effective approach for discovering novel high-performance quadratic NLO materials, particularly those involving organic–inorganic hybrid compounds.

Results and discussion

Crystal structure

Through analysis using single crystal X-ray diffraction techniques, it has been determined that MMTA forms crystals within the polar NCS orthorhombic space group Pn with specific cell parameters: a = 8.6987(5) Å, b = 7.9671(5) Å, c = 13.4081(8) Å, and Z = 2 (Table 1 and S1†). The asymmetric unit of [Mn(CH$_3$CONH$_2$)$_2$][Hg(SCN)$_4$] consists of one Mn atom, one Hg atom, two acetamide molecules and four –S–C≡N– groups.

Table 1 Crystal data and refinement parameters of MMTA

Parameter	MMTA
Empirical formula	[Mn(CH$_3$CONH$_2$)$_2$][Hg(SCN)$_4$]
Radiation λ (Mo Kα) (Å)	0.71073
Molecular weight	605.99
Temperature (K)	296.15
Description	Prism
Color	Colorless
Crystal size (mm)	0.28 × 0.12 × 0.11
Crystal system	Monoclinic
Crystal group	Pn
a (Å)	8.6987(5)
b (Å)	7.9671(5)
c (Å)	13.4081(8)
β/°	90.668(4)
V (Å^3)	929.16(10)
Z	2
Flack parameter	0.016(5)
Final R indices [I > 2σ(I)](R, wR)	R$_1$ = 0.0225, wR$_2$ = 0.0523
R indices (all data) (R, wR)	R$_1$ = 0.0251, wR$_2$ = 0.0537

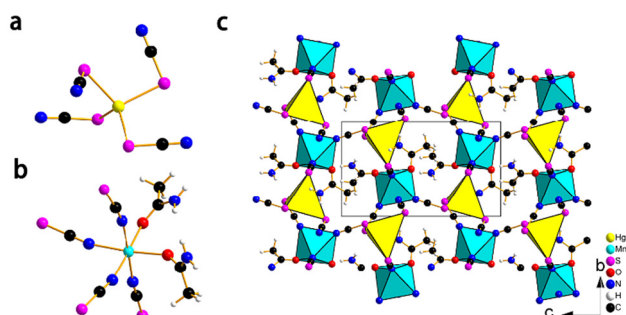$w = [s^2(F_o)^2 + (0.1000P)^2]^{-1}$, where $P = (F_o{}^2 + 2F_c{}^2)/3$.

Fig. 1 (a) Asymmetric octahedral unit [MnN$_4$O$_2$]. (b) Tetrahedral unit [HgS$_4$]. (c) Crystal structure of [Mn(CH$_3$CONH$_2$)$_2$][Hg(SCN)$_4$] viewed along the a-axis. Hydrogen bonding between layers.

As shown in Fig. 1 and S2,† each Hg atom bonds with four S atoms from –S–C≡N– ions to form asymmetric HgS$_4$ tetrahedra. The Hg–S bond length ranges from 2.5179 to 2.5611 Å. Each Mn atom coordinates with four N atoms from –S–C≡N– ions along with two O atoms originating from acetamide molecules to form the highly symmetric octahedral unit [MnN$_4$O$_2$]. The Mn–O bond length ranges from 2.1683 to 2.1704 Å and the Mn–N bond length ranges from 2.2032 to 2.2273 Å. The asymmetric [HgS$_4$] tetrahedra and MnN$_4$O$_2$ octahedra are linked together by four π-conjugated –S–C≡N– ligands, which collectively form an interconnected polar network in three dimensions.

Crystal growth and morphology

The MMTA crystals were grown utilizing a temperature lowering method, while conducting extensive optimization for enhanced crystal growth conditions.[40,41] The initial material undergoes two distinct recrystallization phases to achieve high purity. A slow crystallization phase promotes the growth of seed crystals, which are subsequently carefully selected based

on the desirable morphological characteristics. Large single crystals are obtained by incorporating the selected seed crystals into a saturated solution and employing a controlled cooling method that decreases the temperature by 0.2 degrees daily. Within approximately one month's time frame, high-quality crystals measuring up to dimensions of $50 \times 50 \times 12$ mm^3 were successfully obtained (Fig. 2a). The energy-dispersive spectroscopy (EDS) mapping technique was used to directly reveal the element distribution of the crystal (Fig. S3†). Each element, including Mn, Hg, S, C, N and O, is well distributed in this crystal. The crystals show good thermal stability up to 200 °C (Fig. S4†). The morphological characteristics of these crystals reflect their underlying structure, which predominantly relies on relative growth rates among different facets. It should be emphasized that the observed morphology is significantly influenced by various factors including seed orientation, solvent supersaturation levels, pH values, variations in temperature, presence of impurities, hydrodynamic effects, and cooling rate. In order to precisely determine the actual morphological features exhibited by these grown crystals, PXRD data analysis along with interfacial angle measurements has been carried out (Fig. 2b). The {0 0 2} facet (the largest facet), along with the {0 1 0}, {1 0 1}, and {1 1 0} facets, was formed during the process of crystal growth.
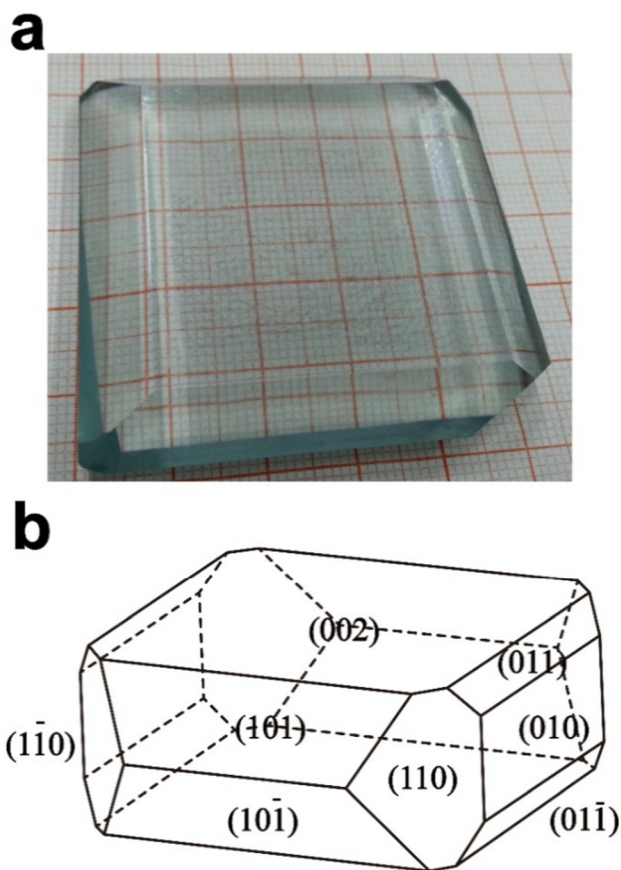
Linear and nonlinear optical properties

As single crystals find extensive use in optical applications, the range of optical transmission and the transparency cutoff are crucial considerations. Fig. 3 displays the UV-Vis-NIR transmission spectrum of the MMTA crystal at room temperature. The results reveal that the MMTA crystal exhibits a wide transmission range spanning from 360 to 2500 nm, with its UV transparency cutoff occurring precisely at 360 nm (equivalent to an energy value of 3.451 eV). Notably, the presence of Mn^{2+} ions leads to the emergence of a distinctive absorption peak at 413 nm (Fig. S5†), which can be attributed to low-energy d–d transitions taking place. Fig. 4 illustrates the SHG behavior observed in powdered MMTA crystals. It is worth noting that as particle size increases, SHG intensity also rises until it reaches a maximum plateau level, indicating type I phase-matchability for MMTA.[42] The comparison between MMTA and KDP in terms of the SHG intensity generated within the
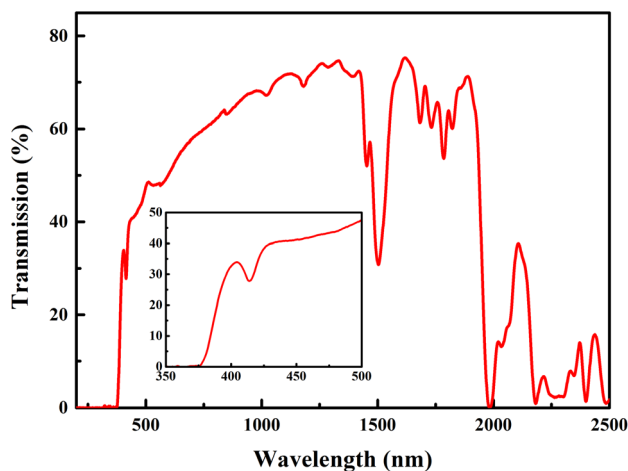

Fig. 3 The UV-Vis-NIR transmittance spectrum of the [Mn(CH$_3$CONH$_2$)$_2$][Hg(SCN)$_4$] crystal measured along the (0 0 1) direction.

Fig. 2 As-grown single crystals of [Mn(CH$_3$CONH$_2$)$_2$][Hg(SCN)$_4$] (a) and typical factual growth morphology (b).

Fig. 4 Phase-matching, that is, particle size *vs.* SHG intensity for [Mn(CH$_3$CONH$_2$)$_2$Hg(SCN)$_4$] and oscilloscope traces of the SHG signals of KDP and [Mn(CH$_3$CONH$_2$)$_2$][Hg(SCN)$_4$].

4308 | *Inorg. Chem. Front.*, 2025, **12**, 4306–4311

This journal is © the Partner Organisations 2025

same particle range indicates that the crystal demonstrates a significantly stronger SHG effect, approximately 2.5 times higher than that of KDP. This level of enhancement is comparable to previously reported findings on organic[43] and organic–inorganic hybrid nonlinear optical materials.[39]

Structure–property relationships

As the structural composition plays a crucial role in determining the functional properties of solid-state materials. Previous studies have indicated that the exceptional NLO and piezoelectric characteristics of MMTA can be attributed to the presence of an asymmetric HgS_4 tetrahedron and MnN_4O_2 octahedron, connected by $–S–C≡N–$ bridges. It is widely acknowledged that the significant macro-SHG response primarily arises from a combination of high micro-hyperpolarizability and favorable crystal packing arrangements.[44] As shown in Fig. 1, the distortions of HgS_4 and MnN_4O_2 polyhedra are relatively large; the combined polarizations resulting from these distorted polyhedra, connected by SCN ligands, contribute significantly to a substantial net dipole moment and polarization. As a result, the remarkable SHG response observed in MMTA may primarily be attributed to the synergistic effect of π-conjugated $–S–C≡N–$ ligands and distorted polyhedra. In addition, in crystals with a polar point group such as MMTA, there exists an inherent direction of spontaneous polarization. The distorted HgS_4 and MnN_4O_2 polyhedra disrupt the alignment of positive and negative charge centers within the crystal lattice, thereby resulting in the formation of electric dipoles and polarization. In order to investigate the mechanism of the large SHG effect observed in MMTA, we conducted an analysis on the maximum SHG tensor components d_{31}. The calculated absolute value of d_{31} at its static limit was found to be 1.158 pm V^{-1}, which aligns remarkably well with the experimentally measured powder SHG effect. By examining the density map for SHG, it becomes evident that the primary contributions originate from localized S 3p and N 2p orbitals, while there is a minor involvement of Mn 3d orbitals in the valence band (VB) and Hg 6s, S 3p, and N 2p orbitals in the conduction band (CB) (Fig. 5 and S6†). The birefringence of the
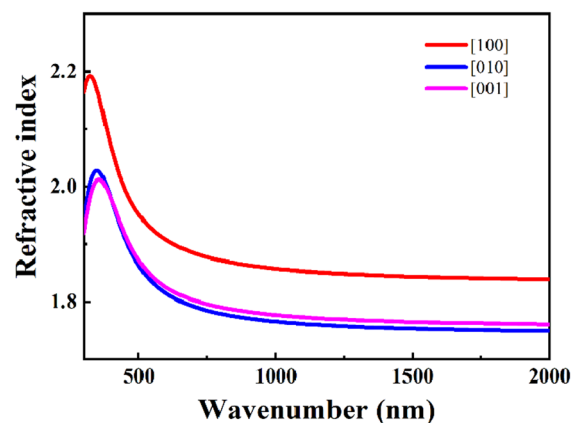

Fig. 6 The calculated refractive index and birefringence for [Mn(CH$_3$CONH$_2$)$_2$][Hg(SCN)$_4$] along different directions.

MMTA crystal was also calculated, as it is a crucial parameter for determining the phase-matching range. It can be observed from Fig. 6 that the calculated birefringence Δn for MMTA ranges from approximately 0.09 to 0.12, indicating a moderate level of birefringence in the crystal. This moderate value of Δn aligns well with the experimental phase-matching behavior. As deduced from the calculations of the electronic structure, the remarkable optical characteristics of MMTA can primarily be attributed to the synergistic interaction between extensively distorted polyhedra and π-conjugated $–S–C≡N–$ ligands.

Conclusions

In summary, we have successfully synthesized a polar hybrid organometallic compound called MMTA, which combines organic and inorganic components. By employing a temperature reduction method, we were able to grow inch-sized single crystals of MMTA. Furthermore, MMTA exhibits wide optical transparency and demonstrates impressive phase-matchable NLO properties with a second harmonic generation (SHG) response equivalent to 2.5 times that of KDP. Theoretical calculations indicate that the exceptional optical properties of MMTA primarily stem from the collaborative influence of π-conjugated $–S–C≡N–$ ligands and highly distorted polyhedra. This study presents an exciting avenue for further exploration into organic–inorganic hybrid materials with outstanding NLO performance.

Author contributions

Fig. 5 The SHG density of d_{31} in the VB (a) and the CB (b) for [Mn(CH$_3$CONH$_2$)$_2$][Hg(SCN)$_4$].

Peiqing Long: design of the study, data collection and analysis, and writing – original draft. Chunli Hu: resources and project administration. Xitao Liu: supervision and data analysis. Jianggao Mao: resources, project administration, writing – review & editing, and supervision.
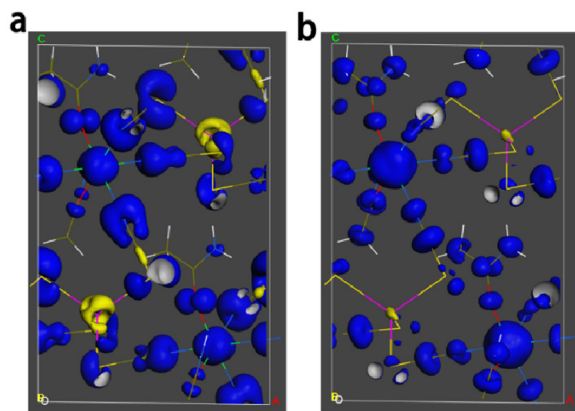
This journal is © the Partner Organisations 2025

Inorg. Chem. Front., 2025, **12**, 4306–4311 | **4309**

Data availability

The data that support the findings of this study are available from the corresponding author upon reasonable request.

Conflicts of interest

There are no conflicts to declare.

Acknowledgements

References

1 M. Mutailipu, J. Han, Z. Li, F. Li, J. Li, F. Zhang, X. Long, Z. Yang and S. Pan, Achieving the full-wavelength phase-matching for efficient nonlinear optical frequency conversion in $C(NH_2)3BF_4$, *Nat. Photonics*, 2023, **17**, 694–701.

2 M. Mutailipu, K. R. Poeppelmeier and S. Pan, Borates: A Rich Source for Optical Materials, *Chem. Rev.*, 2021, **121**, 1130–1202.

3 Y. Kang, C. Yang, J. Gou, Y. Zhu, Q. Zhu, W. Xu and Q. Wu, From $Cd(SCN)_2(CH_4N_2S)_2$ to $Cd(SCN)_2(C_4H_6N_2)_2$: Controlling Sulfur Content in Thiocyanate Systems Significantly Improves the Overall Performance of UV Nonlinear Optical Materials, *Angew. Chem., Int. Ed.*, 2024, **63**, e202402086.

4 V. G. Dmitriev, G. G. Gurzadyan and D. N. Nicogosyan, *Handbook of Nonlinear Optical Crystals*, Springer-Verlag, New York, 1999.

5 D. Nikogosyan, *Nonlinear Optical Crystals: A Complete Survey*, Springer Science & Business Media, 2006.

6 C. Y. Pan, X. R. Yang, L. Xiong, Z. W. Lu, B. Y. Zhen, X. Sui, X. B. Deng, L. Chen and L. M. Wu, Solid-State Nonlinear Optical Switch with the Widest Switching Temperature Range Owing to Its Continuously Tunable T_c, *J. Am. Chem. Soc.*, 2020, **142**, 6423–6431.

7 Y. Li, Z. Zhou, S. Zhao, F. Liang, Q. Ding, J. Sun, Z. Lin, M. Hong and J. Luo, A Deep-UV Nonlinear Optical Borosulfate with Incommensurate Modulations, *Angew. Chem., Int. Ed.*, 2021, **60**, 11457–11463.

8 J. Wang, Y. Cheng, H. Wu, Z. Hu, J. Wang, Y. Wu and H. Yu, Sr3 $[SnOSe_3][CO_3]$: A Heteroanionic Nonlinear Optical Material Containing Planar pi-conjugated $[CO_3]$ and Heteroleptic $[SnOSe_3]$ Anionic Groups, *Angew. Chem., Int. Ed.*, 2022, **61**, e202201616.

9 F. Ding, K. J. Griffith, W. Zhang, S. Cui, C. Zhang, Y. Wang, K. Kamp, H. Yu, P. S. Halasyamani, Z. Yang, S. Pan and K. R. Poeppelmeier, $NaRb_6(B_4O_5(OH)_4)_3(BO_2)$ Featuring Noncentrosymmetry, Chirality, and the Linear Anionic Group BO_2^-, *J. Am. Chem. Soc.*, 2023, **145**, 4928–4933.

10 J. Cheng, G. Yi, Z. Zhang, Y. Long, H. Zeng, L. Huang, G. Zou and Z. Lin, In Situ Chiral Template Approach to Synthesize Homochiral Lead Iodides for Second-Harmonic Generation, *Angew. Chem., Int. Ed.*, 2024, **63**, e202318385.

11 J. Chen, C. L. Hu, F. Kong and J. G. Mao, High-Performance Second-Harmonic-Generation (SHG) Materials: New Developments and New Strategies, *Acc. Chem. Res.*, 2021, **54**, 2775–2783.

12 X. Liu, Y. C. Yang, M. Y. Li, L. Chen and L. M. Wu, Anisotropic structure building unit involving diverse chemical bonds: a new opportunity for high-performance second-order NLO materials, *Chem. Soc. Rev.*, 2023, **52**, 8699–8720.

13 J. Guo, J. Huang, A. Tudi, X. Hou, S. Han, Z. Yang and S. Pan, Birefringence Regulation by Clarifying the Relationship Between Stereochemically Active Lone Pairs and Optical Anisotropy in Tin-based Ternary Halides, *Angew. Chem., Int. Ed.*, 2023, **62**, e202304238.

14 H. Liu, Q. Wu, L. Liu, Z. Lin, P. S. Halasyamani, X. Chen and J. Qin, $AgBi(SO_4)(IO_3)_2$: Aliovalent Substitution Induces Structure Dimensional Upgrade and Second Harmonic Generation Enhancement, *Chem. Commun.*, 2021, **57**, 3712–3715.

15 H. Qiu, F. Li, Z. Li, Z. Yang, S. Pan and M. Mutailipu, Breaking the Inherent Interarrangement of $[B_3O_6]$ Clusters for Nonlinear Optics with Orbital Hybridization Enhancement, *J. Am. Chem. Soc.*, 2023, **145**, 24401–24407.

16 P. J. Kim, M. Jazbinsek and O. P. Kwon, Selective Growth of Highly Efficient Electrooptic Stilbazolium Crystals by Sequential Crystal Growth in Different Solvents, *Cryst. Growth Des.*, 2011, **11**, 3060–3064.

17 E. Y. Choi, P. J. Kim, M. Jazbinsek, J. T. Kim, Y. S. Lee, P. Günter, S. W. Lee and O. P. Kwon, 4-Nitrophenylhydrazone Crystals with Large Quadratic Nonlinear Optical Response by Optimal Molecular Packing, *Cryst. Growth Des.*, 2011, **11**, 3049–3055.

18 P. J. Kim, J. H. Jeong, M. Jazbinsek, S. B. Choi, I. H. Baek, J. T. Kim, F. Rotermund, H. Yun, Y. S. Lee, P. Günter and O. P. Kwon, Highly Efficient Organic THz Generator Pumped at Near-Infrared: Quinolinium Single Crystals, *Adv. Funct. Mater.*, 2012, **22**, 200–209.

19 S. Zhao, X. Yang, Y. Yang, X. Kuang, F. Lu, P. Shan, Z. Sun, Z. Lin, M. Hong and J. Luo, Non-Centrosymmetric $RbNaMgP_2O_7$ with Unprecedented Thermo-Induced Enhancement of Second Harmonic Generation, *J. Am. Chem. Soc.*, 2018, **140**, 1592–1595.

20 P. F. Li, C. L. Hu, Y. F. Li, J. G. Mao and F. Kong, $Hg_4(Te_2O_5)(SO_4)$: A Giant Birefringent Sulfate Crystal Triggered by a Highly Selective Cation, *J. Am. Chem. Soc.*, 2024, **146**, 7868–7874.

21 J. L. Song, C. L. Hu, X. Xu, F. Kong and J. G. Mao, A Facile Synthetic Route to a New SHG Material with Two Types of Parallel π-Conjugated Planar Triangular Units, *Angew. Chem., Int. Ed.*, 2015, **54**, 3679–3682.

22 P. F. Li, C. L. Hu, F. Kong and J. G. Mao, The First UV Nonlinear Optical Selenite Material: Fluorination Control

4310 | *Inorg. Chem. Front.*, 2025, **12**, 4306–4311

This journal is © the Partner Organisations 2025

in CaYF(SeO$_3$)$_2$ and Y3F(SeO$_3$)$_4$, *Angew. Chem., Int. Ed.*, 2023, **62**, e202301420.

23 J. Lu, Y. K. Lian, L. Xiong, Q. R. Wu, M. Zhao, K. X. Shi, L. Chen and L. M. Wu, How To Maximize Birefringence and Nonlinearity of π-Conjugated Cyanurates, *J. Am. Chem. Soc.*, 2019, **141**, 16151–16159.

24 S. Zhang, L. Jin, Y. Lu, L. Zhang, J. Yang, Q. Zhao, D. Sun, J. J. P. Thompson, B. Yuan, K. Ma, Akriti, J. Y. Park, Y. H. Lee, Z. Wei, B. P. Finkenauer, D. D. Blach, S. Kumar, H. Peng, A. Mannodi-Kanakkithodi, Y. Yu, E. Malic, G. Lu, L. Dou and L. Huang, Moiré superlattices in twisted two-dimensional halide perovskites, *Nat. Mater.*, 2024, **23**, 1222–1229.

25 J. Sun, K. Wang, K. Ma, J. Y. Park, Z. Y. Lin, B. M. Savoie and L. Dou, Emerging Two-Dimensional Organic Semiconductor-Incorporated Perovskites horizontal line A Fascinating Family of Hybrid Electronic Materials, *J. Am. Chem. Soc.*, 2023, **145**, 20694–20715.

26 J. Xu, X. Li, J. Xiong, C. Yuan, S. Semin, T. Rasing and X. H. Bu, Halide Perovskites for Nonlinear Optics, *Adv. Mater.*, 2019, **32**, e1806736.

27 M. Simenas, A. Gagor, J. Banys and M. Maczka, Phase Transitions and Dynamics in Mixed Three- and Low-Dimensional Lead Halide Perovskites, *Chem. Rev.*, 2024, **124**, 2281–2326.

28 X. K. Liu, W. Xu, S. Bai, Y. Jin, J. Wang, R. H. Friend and F. Gao, Metal halide perovskites for light-emitting diodes, *Nat. Mater.*, 2021, **20**, 10–21.

29 J. C. Blancon, J. Even, C. C. Stoumpos, M. G. Kanatzidis and A. D. Mohite, Semiconductor physics of organic-inorganic 2D halide perovskites, *Nat. Nanotechnol.*, 2020, **15**, 969–985.

30 L. R. Mingabudinova, V. V. Vinogradov, V. A. Milichko, E. Hey-Hawkins and A. V. Vinogradov, Metal-organic frameworks as competitive materials for non-linear optics, *Chem. Soc. Rev.*, 2016, **45**, 5408–5431.

31 X. Liu, P. Long, X. Wang, Z. Gao, Y. Lü and Z. Yi, Efficient Raman scattering response and large piezoelectricity in noncentrosymmetric MnHg(SCN)$_4$ crystals, *J. Mater. Chem. C*, 2017, **5**, 3238–3246.

32 D. R. Yuan, D. Xu, M. G. Liu, F. Qi, W. T. Yu, W. B. Hou, Y. H. Bing, S. Y. Sun and M. H. Jiang, Structure and properties of a complex crystal for laser diode frequency doubling: Cadmium mercury thiocyanate, *Appl. Phys. Lett.*, 1997, **70**, 544–546.

33 M. H. Jiang and Q. Fang, Organic and Semiorganic Nonlinear Optical Materials, *Adv. Mater.*, 1999, **11**, 1147–1151.

34 X. Q. Wang, D. Xu, M. K. Lu, D. R. Yuan, X. Yin, G. H. Zhang, S. X. Xu, G. W. Lu, C. F. Song, S. Y. Guo, J. R. Liu, G. Y. Zhou, D. Wang, Z. H. Yang, X. Zhao, Q. Ren, J. Q. Zhao and W. L. Liu, Crystal growth and physical properties of UV nonlinear optical crystal zinc cadmium thiocyanate, ZnCd(SCN)$_4$, *Chem. Phys. Lett.*, 2001, **346**, 393–406.

35 G. H. Zhang, D. Xu, M. K. Lu, D. R. Yuan, X. Q. Wang, F. Q. Meng, S. Y. Guo, Q. Ren and M. H. Jiang, Violet light generation by frequency doubling of GaAlAs diode laser using a metallo-organic complex crystal ZnCd(SCN)$_4$, *Opt. Laser Technol.*, 2001, **33**, 121–124.

36 X. Q. Wang, D. Xu, M. K. Lu, D. R. Yuan, J. Huang, X. F. Cheng, T. X. Xie, G. H. Zhang, S. L. Wang, S. Y. Guo, J. R. Liu, Z. H. Yang and P. Wang, Growth and characterization of a novel UV nonlinear optical crystal: MnHg(SCN)$_4$(H$_2$O)$_2$·2C$_4$H$_9$NO, *J. Cryst. Growth*, 2002, **234**, 469–479.

37 X. Q. Wang, D. Xu, M. K. Lu, D. R. Yuan, J. Huang, X. F. Cheng, S. L. Wang, S. Y. Guo, G. H. Zhang, M. Pan, X. L. Duan and Z. H. Yang, Crystal growth and characterization of a new organometallic nonlinear-optical crystal material : MnHg(SCN)$_4$(C$_3$H$_8$O$_2$), *Phys. Status Solidi A*, 2002, **191**, 106–116.

38 X. Q. Wang, D. Xu, M. K. Lu, D. R. Yuan, X. F. Cheng, J. Huang, S. L. Wang, W. T. Yu, H. Q. Sun, X. L. Duan, Q. Ren and H. L. Yang, Growth morphology and thermal properties of the organometallic nonlinear optical crystal: MnHg(SCN)$_4$(C$_2$H$_6$OS)$_2$, *Chem. Phys. Lett.*, 2003, **367**, 230–237.

39 X. T. Liu, X. Q. Wang, X. J. Lin, G. H. Sun, G. H. Zhang and D. Xu, Growth, Characterization and Theoretical Study of a Novel Organometallic Nonlinear Optical Crystal: CdHg(SCN)$_4$(C2H5NO)$_2$, *Appl. Phys. A*, 2012, **107**, 949–957.

40 A. Suresh, R. M. Jauhar, T. C. S. Girisun, N. Manikandan and G. Vinitha, Third order nonlinearity examined by pulsed and CW lasers: an organic urea barbituric acid (UBA) single crystal for optical limiting application with DFT study, *Mater. Res. Express*, 2024, **11**, 016203.

41 T. S. Girisun and S. Dhanuskodi, Linear and nonlinear optical properties of tris thiourea zinc sulphate single crystals, *Cryst. Res. Technol.*, 2009, **44**, 1297–1302.

42 S. K. Kurtz and T. T. Perry, A Powder Technique for the Evaluation of Nonlinear Optical Materials, *J. Appl. Phys.*, 1968, **39**, 3798–3813.

43 T. C. Sabari Girisun and S. Dhanuskodi, Nonlinear optical susceptibilities of diglycinyl thiourea for frequency conversion and optical limiting applications, *Chem. Phys. Lett.*, 2010, **491**, 248–253.

44 D. S. Chemla and J. Zyss, *Nonlinear optical properties of organic molecules and crystals*, Academic Press, 1987.

This journal is © the Partner Organisations 2025

Inorg. Chem. Front., 2025, **12**, 4306–4311 | **4311**